Two-component density functional theory calculations of positron lifetimes for small vacancy clusters in silicon

D. V. Makhov and Laurent J. Lewis
Département de physique et Regroupement québécois sur les matériaux de pointe (RQMP) Université de Montréal, Case Postale 6128, Succursale Centre-Ville, Montréal, Québec H3C 3J7, Canada
(Received 8 February 2005; published 31 May 2005; publisher error corrected 7 June 2005)

The positron lifetimes for various vacancy clusters in silicon are calculated within the framework of the two-component electron-positron density functional theory. The effect of the trapped positron on the electron density and on the relaxation of the structure is investigated. Our calculations show that, contrary to the usual assumption, the positron-induced forces do not compensate in general for electronic inward forces. Thus, geometry optimization is required in order to determine positron lifetime accurately. For the monovacancy and the divacancy, the results of our calculations are in good agreement with the experimental positron lifetimes, suggesting that this approach gives good estimates of positron lifetimes for larger vacancy clusters, required for their correct identification with positron annihilation spectroscopy. As an application, our calculations show that fourfold trivacancies and symmetric fourfold tetravacancies have positron lifetimes similar to monovacancies and divacancies, respectively, and can thus be confused in the interpretation of positron annihilation experiments.

DOI: 10.1103/PhysRevB.71.205215 PACS number(s): 71.60.+z, 78.70.Bj, 71.55.Cn, 61.72.Bb

I. INTRODUCTION

Silicon always contains a certain number of defects that significantly influence its electrical and optical properties. Vacancies and their clusters are one of the basic defect types. They are usually created by irradiation of silicon with, e.g., electrons[1–3] or neutrons,[4–6] but can also be present in as-grown samples.[7]

One of the most powerful experimental tool for probing defects in crystalline materials is positron annihilation spectroscopy (PAS). However, the correct identification of defects with PAS requires the knowledge of accurate positron lifetimes for the various kinds of defects, which can be provided by numerical calculations. In most studies, positron lifetimes are calculated using the simple practical method proposed by Puska and Nieminen[8,9] where the electron and positron densities are determined without imposing self-consistency; we will refer to this as the nonself-consistent (NSC) method. In this method, the electron density is first calculated without including the positron (or just taken as a superposition of free-atom electron densities[8]). Next, the positron density is calculated by solving the one-particle Schrödinger equation using an effective potential which includes the Coulomb potential and the electron-positron correlation potential determined from the local electron density. This method provides reasonable agreement with experimental positron lifetimes for bulk metals[10,11] and semiconductors[11] where the positron density is low due to delocalization. However, in the case of defects, the trapped positron can have a significant impact on the nearby electron density and lattice relaxation. In the case of vacancy clusters, the latter effect is usually taken into account by performing calculations using the unrelaxed geometries:[12] It is assumed that positron-induced outward forces approximately compensate for electronic inward forces on the atoms around the defects. Obviously, the precision of such calculations is not perfect. Moreover, for some kinds of defects, like fourfold vacancy clusters,[13] the unrelaxed geometry is simply not defined.

A more precise approach to positron lifetime calculations is two-component density functional theory (DFT).[14,15] In this case, electron and positron densities are optimized self-consistently. This significantly complicates the computational procedure but, on the other hand, allows positron-induced forces to be accurately calculated and, therefore, the relaxed geometries of defects with positrons trapped inside to be properly determined. In this work, we use the two-component DFT to calculate positron lifetimes for small vacancy clusters in silicon in both "part-of-a-hexagonal-ring" (PHR) and fourfold configurations.[13]

II. THEORY

In positron annihilation measurements, the intensity of the positron beam is relatively low. As a result, only one positron at a time is usually trapped by a defect. We thus consider a single positron interacting with the electron gas. In the framework of DFT, the total energy of the system is written as

$$E[n_e,n_p] = T[n_e] + T[n_p] + \int d\mathbf{r} V_{\text{ext}}(\mathbf{r})[n_p(\mathbf{r}) - n_e(\mathbf{r})] - \int d\mathbf{r} \int d\mathbf{r}' \frac{n_p(\mathbf{r})n_e(\mathbf{r}')}{|\mathbf{r}-\mathbf{r}'|} + E_{xc}[n_e] + E_{e-p}[n_e,n_p], \quad (1)$$

where n_e and n_p are the electron and positron densities, $T[n]$ and $E_{xc}[n]$ are the kinetic energy and exchange-correlation functionals, respectively, V_{ext} is an external potential (due to the ions), and $E_{e-p}[n_e,n_p]$ is the electron-positron correlation functional. As in the usual one-component DFT, the minimum of this total energy functional can be determined by solving a set of Kohn-Sham equations for the electrons and the positron

$$-\tfrac{1}{2}\nabla^2\psi_i(\mathbf{r}) + [-V_{\text{ext}}(\mathbf{r}) + V_h^e(\mathbf{r}) + V_{xc}(\mathbf{r}) + V_{e-p}^e(\mathbf{r})]\psi_i(\mathbf{r}) = \epsilon_i\psi_i(\mathbf{r}), \tag{2}$$

$$-\tfrac{1}{2}\nabla^2\psi_p(\mathbf{r}) + [V_{\text{ext}}(\mathbf{r}) + V_h^p(\mathbf{r}) + V_{e-p}^p(\mathbf{r})]\psi_p(\mathbf{r}) = \epsilon_p\psi_p(\mathbf{r}), \tag{3}$$

where $V_h^e(\mathbf{r})$ and $V_h^p(\mathbf{r})$ are the Hartree potentials for the electrons and the positron, respectively (we explicitly exclude the positron self-interaction here)

$$V_h^e(\mathbf{r}) = \int d\mathbf{r}' \frac{n_e(\mathbf{r}') - n_p(\mathbf{r}')}{|\mathbf{r} - \mathbf{r}'|}, \tag{4}$$

$$V_h^p(\mathbf{r}) = \int d\mathbf{r}' \frac{-n_e(\mathbf{r}')}{|\mathbf{r} - \mathbf{r}'|}. \tag{5}$$

$V_{xc}(\mathbf{r})$ is the exchange-correlation potential

$$V_{xc}(\mathbf{r}) = \frac{\delta E_{xc}[n_e]}{\delta n_e(\mathbf{r})}, \tag{6}$$

and $V_{e-p}^e(\mathbf{r})$ and $V_{e-p}^p(\mathbf{r})$ are the electron-positron correlation potentials for the electrons and the positron, respectively,

$$V_{e-p}^e(\mathbf{r}) = \frac{\delta E_{e-p}[n_e, n_p]}{\delta n_e(\mathbf{r})}, \tag{7}$$

$$V_{e-p}^p(\mathbf{r}) = \frac{\delta E_{e-p}[n_e, n_p]}{\delta n_p(\mathbf{r})}. \tag{8}$$

When the electron and positron densities are known, the annihilation rate λ can easily be found as

$$\lambda = \pi r_e^2 c \int d\mathbf{r}\, \gamma(n_e) n_e(\mathbf{r}) n_p(\mathbf{r}), \tag{9}$$

where r_e is the classical radius of the electron, c is the speed of light, and γ is an enhancement factor reflecting the increase of electron density in the vicinity of the positron due to electron-positron correlations.

The correct treatment of electron-positron correlations is the most conjectural part of two-component DFT calculations. While the wide use of (one-component) DFT has inspired a lot of research on electron-electron exchange-correlation functionals over the last decades, the commonly used electron-positron correlation functional is based on 25 years old calculations by Arponen and Pajanne[16] for a single positron in a uniform electron gas. The parametrization of these results by Boroński and Nieminen[14] provides the correlation potential V_{e-p} and the interpolation formula for the enhancement factor $\gamma(n_e)$ in the limit of an infinitely small positron density

$$V_{e-p}[\text{Ry}] = \begin{cases} -1.56/\sqrt{r_s} + (0.051 \ln r_s - 0.081)\ln r_s + 1.14; & r_s \leqslant 0.302 \\ -0.92305 - \dfrac{0.05459}{r_s^2}; & 0.302 \leqslant r_s \leqslant 0.56 \\ -0.6298 - \dfrac{13.15111}{(r_s + 2.5)^2} + \dfrac{2.8655}{(r_s + 2.5)}; & 0.56 \leqslant r_s \leqslant 8.0 \\ -0.524 - 179856.2768 n_e^2 + 186.4207 n_e; & r_s \geqslant 8.0, \end{cases} \tag{10}$$

and

$$\gamma(n_e) = 1 + 1.23 r_s + 0.8295 r_s^{3/2} - 1.26 r_s^2 + 0.3286 r_s^{5/2} + (1/6) r_s^3, \tag{11}$$

where $r_s = [(4/3)\pi n_e]^{-1/3}$ is in atomic units.

The use of the correlation potential (10) is justified in the case of bulk materials, where the positron is delocalized. However, in the case of defects, the positrons are localized and the positron density is usually comparable to, or higher than, the electron density; the dependence of V_{e-p} on n_p can thus play a significant role. Puska, Seitsonen, and Nieminen[17] have considered a more advanced functional based on the calculations by Lantto[18] for a uniform electron-positron liquid with various electron and positron densities. However, they have found, in the case of the Ga vacancy in GaAs, that this functional significantly overestimates the delocalization of the positron, and fails to reproduce correctly the lattice relaxation around the defect. We have obtained similar results in the case of vacancy clusters in silicon.[19] The most probable reason for this state of affairs is that the positron-positron interactions that are present in the electron-positron liquid do not exist in the case of a single localized positron. On the other hand, the functional (10) has been shown to provide reasonable results even for positrons trapped in defects.[20,21] Taking these considerations into account, we have decided to use this functional in our calculations; nevertheless, it remains an important challenge to develop a proper correlation functional for a single localized positron in the electron gas.

III. RESULTS AND DISCUSSION

The calculations were performed using the Vienna *Ab-initio* Simulation Package (VASP), which employs

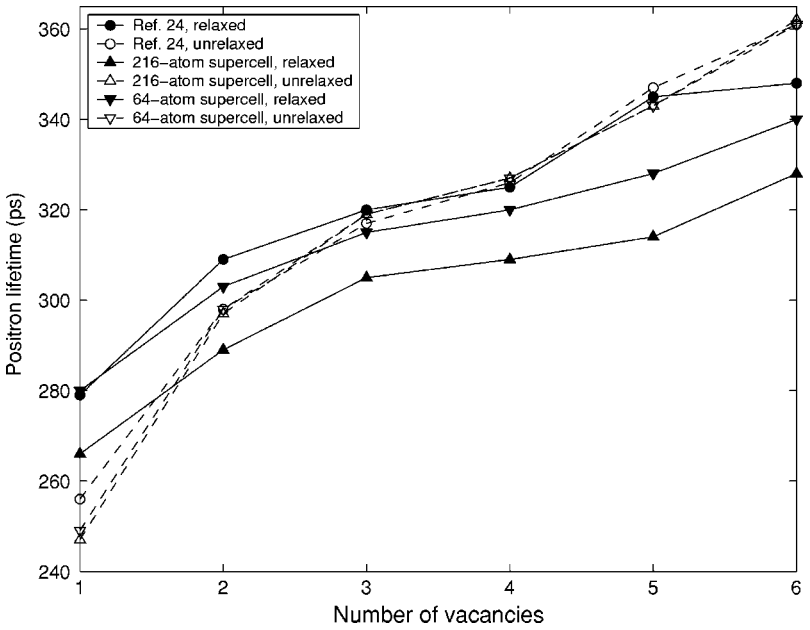

FIG. 1. Calculated positron lifetimes for vacancy clusters in the PHR configurations in silicon (chain configuration for V_4): two-component DFT with 216-atom and 64-atom supercells [without semiconductor correction (Ref. 25)] and results from Ref. 24 (64-atom supercell), for both relaxed (solid lines) and unrelaxed (dashed lines) geometries.

pseudopotential DFT with the projector augmented-wave method (PAW).[22,23] The code has been modified in order to calculate self-consistently the electron and positron wave functions. As external potential for the positron, the local part of the pseudopotential has been employed. We used the local-density approximation (LDA) for both the electron exchange-correlation and the electron-positron correlation functionals. The latter has been taken in the low positron density limit [Eq. (10)]. Most calculations have been performed using a 216-atom supercell and an energy cutoff of 18 Ry; given the large size of the supercell, Brillouin zone sampling has been restricted to the Γ point.

The calculated positron lifetimes for vacancy clusters in the PHR/chain configurations, both with and without lattice relaxation, are displayed in Fig. 1. For comparison, we also show the results of Saito and Oshiyama,[24] who performed similar calculations using two-component DFT with norm-conserving pseudopotentials and a 64-atom supercell. One can see that, for the unrelaxed geometries, our results are very close to those of Ref. 24; for the relaxed geometries however, our calculations give positron lifetimes which are 15–30 ps lower than those reported in Ref. 24. We note that, according to Saito and Oshiyama, positron-induced forces prevail in the case of the divacancy, causing an outward relaxation of the lattice and, therefore, an increase of the positron lifetime; in contrast, our calculations show an inward relaxation causing a decrease of the lifetime.

In order to understand this difference, we have performed additional calculations for a 64-atom supercell. The results are also plotted in Fig. 1. One can see that, whereas the size of the supercell does not significantly affect the calculated positron lifetimes for fixed geometries, it has a strong effect when lattice relaxation is taken into account: For calculations with full geometry optimization, positron lifetimes calculated in the 64-atom supercell are substantially higher than the corresponding values in the 216-atom supercell and, for most defects, are rather close to the results of Saito and Oshiyama. In order to determine whether a 216-atom supercell is sufficient, calculations for some vacancy clusters have also been carried out for a 512-atom supercell and lower energy cutoff (13.5 Ry). We have found that lifetimes in the latter case are just 3–5 ps lower, and that this difference decreases to 2–3 ps when the same low cutoff is used with the 216-atom supercell. One can therefore conclude that the results for the 216-atom supercell are essentially converged.

Our results thus show that calculations with the NSC method for unrelaxed geometries provide only approximate estimates of the actual positron lifetimes. One can see from Fig. 1 that, contrary to the usual assumption (which is based on Saito and Oshiyama's calculations[24]), the positron-induced forces *do not* generally compensate for inward electronic forces, and the effect of lattice relaxation on positron lifetimes significantly depends on the size of the defect. Thus, two-component DFT calculations are necessary for the correct identification of defects with PAS.

Along with the lattice relaxation, the effect of the positron on the electron density around the defect also plays a role, even in the case of fixed geometries. Figure 2 presents a comparison of positron lifetimes calculated for unrelaxed geometries with the two-component DFT and with the NSC method. One can see that the positron lifetime given by the two-component DFT is about 10 ps larger than for the NSC method, i.e., the attraction of the electron density by the localized positron leads, surprisingly, to a decrease of the annihilation rate. In order to explain this phenomenon, we plot in Fig. 3 the average electron and positron densities as a function of distance from the center of the defect

$$\overline{n}(l) = \frac{1}{4\pi l^2}\frac{d}{dl}\int_{|\mathbf{r}-\mathbf{r}_0|<l} d\mathbf{r} n(\mathbf{r}). \tag{12}$$

The calculations show that, as one would expect, the electron density in the center of the defect is higher for the two-component DFT, i.e., the interaction with the positron indeed attracts electron density to the defect. However, at the same time, this increase in the negative charge density deepens the

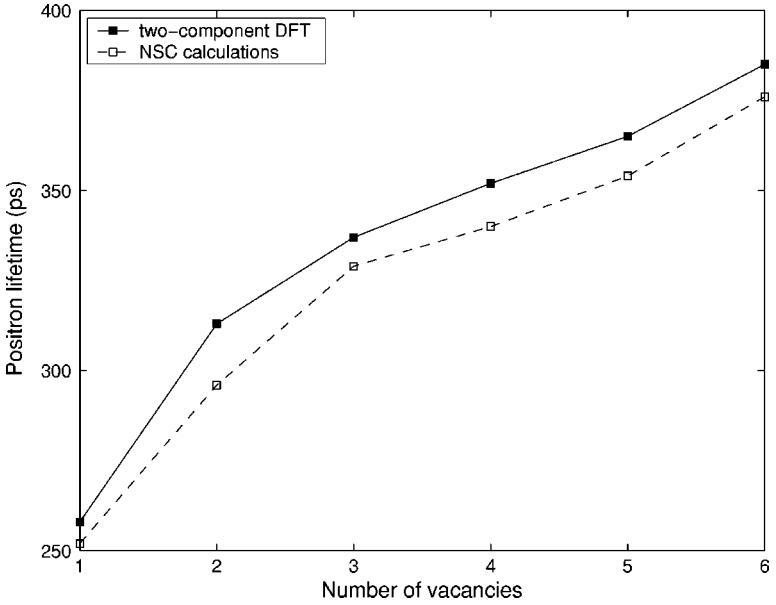

FIG. 2. Calculated positron lifetimes for vacancy clusters in the PHR configurations (chain configuration for V_4) in silicon using two-component DFT (solid line) and NSC method (dashed line).

potential well for the positron. As a result, as one can see from Fig. 3, the positron becomes more localized inside the defect, in a low electron density region. Because annihilation mostly takes place outside the defect, where electron density is high, this enhanced localization leads to the increase in positron lifetimes shown in Fig. 2.

The results of our positron lifetime calculations for the PHR and the fourfold vacancy clusters in silicon are summarized in Table I. For comparison, we also provide the results of our earlier calculations[13] using the NSC method, as well as the experimental lifetimes for the monovacancy and the divacancy.[3] Results are given for calculations both with and without the semiconductor correction[25] to the enhancement factor (11), which reflects the imperfect screening of positrons in semiconductors (see the review by Puska and Nieminen[15] for details). Table I shows that the NSC method underestimates the positron lifetimes for the monovacancy and the divacancy (by 10% and 3%, respectively), and overestimates them for all other clusters. The most significant difference between two-component DFT and NSC results is for the fourfold trivacancy (+12%), the monovacancy (−10%), and the symmetric fourfold tetravacancy (+8%).

One can see that the two-component DFT (with semiconductor correction) gives positron lifetimes which are in very good agreement with the experimental values, significantly better than NSC calculations. Moreover, the two-component DFT method reproduces much better the difference between vacancy and divacancy lifetimes than the NSC method: 25 and 44 ps, respectively, versus 28 ps in the experiment. This suggests that the two-component DFT approach also provides more accurate estimates for positron lifetimes associated with larger vacancy clusters.

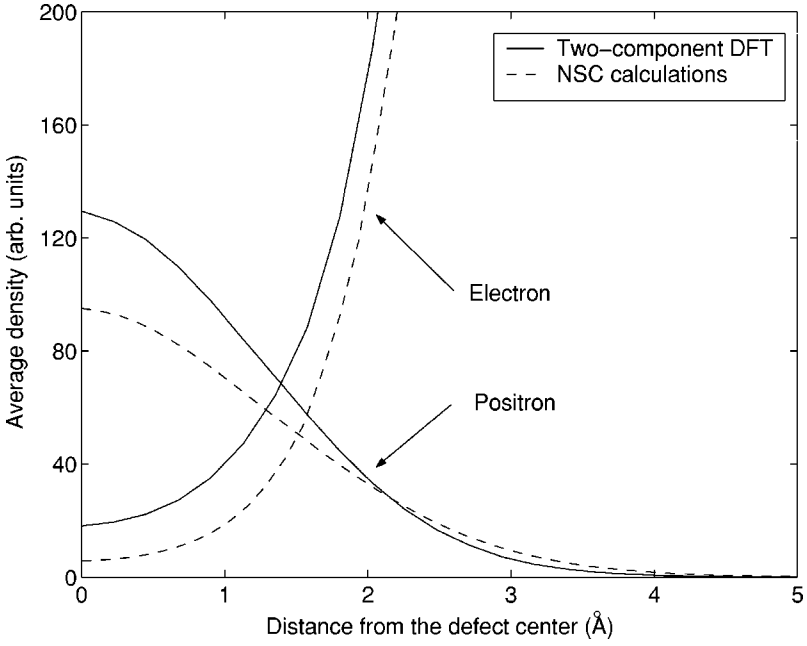

FIG. 3. Calculated average electron and positron densities $\bar{n}$ around the ring hexavacancy in silicon.

TABLE I. Positron lifetimes (in ps) for various vacancy clusters in silicon calculated using the two-component DFT and the NSC method, and experimental data (Ref. 3). The results of the two-component DFT calculations are for fully optimized geometries; the results for the NSC method are given for unrelaxed geometries (see text). Numbers in brackets show the results of two-component DFT calculations without the semiconductor correction (Ref. 25).

Number of vacancies	Two-component DFT	NSC method (unrelaxed)	Experiment[a]
1	280 (267)	252	282
2	305 (290)	296	310
3 PHR	322 (305)	329	
3 fourfold	287 (274)	321	
4 PHR	334 (316)	340	
4 chain	328 (310)	343	
4 fourfold, symm	316 (300)	342	
4 fourfold, nonsymm	330 (312)	347	
5 PHR	333 (315)	354	
5 fourfold	341 (322)	363	
6	347 (328)	376	

[a]Reference 3.

According to the present calculations, fourfold trivacancies and monovacancies have similar positron lifetimes (287 and 280 ps, respectively), and thus can be confused in the interpretation of positron annihilation experiments. In particular, defects having a positron lifetime of 260–300 ps and possessing high thermal stability were observed by Wang *et al.*[26] in plastically deformed silicon and associated to dislocation-bound monovacancies. Our calculations indicate that it can be likewise the signal of the fourfold trivacancies.

In a previous paper[13] we suggested, based on NSC calculations, that the formation of fourfold trivacancies could be responsible for the apparent disagreement between positron lifetime and infrared spectroscopy data reported by Poirier *et al.*:[27] In the process of divacancy annealing, the infrared absorption (associated with divacancies) disappears with time while the positron lifetime remains virtually unchanged. However, the more accurate positron lifetimes reported here suggest that symmetric fourfold tetravacancies, rather than trivacancies, are responsible for this effect: Indeed, the lifetime for fourfold tetravacancies is just slightly higher than that for divacancies (316 ps versus 305 ps). Furthermore, fourfold tetravacancies are optically inactive (like all fourfold clusters), and can easily form from two-parallel divacancies (see Ref. 13 for details). All these considerations point to the formation of symmetric fourfold tetravacancies as the most probable explanation of the observations reported in Ref. 27. However, more measurements with other experimental techniques (e.g., deep level transient spectroscopy) are required in order to confirm this interpretation.

IV. CONCLUSION

We have calculated the positron lifetimes for various PHR and fourfold vacancy clusters in silicon using electron-positron two-component DFT with a 216-atom supercell. It has been found that the results for the monovacancy and the divacancy are in good agreement with the experimental lifetimes reported in Ref. 3.

Contrary to the usual assumption, our calculations show that positron-induced forces generally do not compensate for electronic inward forces. Thus, the use of unrelaxed defect geometries for positron lifetime calculations is not generally justified, and full geometry optimization (with respect to both electronic and positronic forces) is necessary. Furthermore, we have found that the lattice relaxation significantly depends on the size of the supercell; a supercell of at least 216 atoms is required in order to calculate positron lifetimes accurately, even for relatively small defects.

For the two-component DFT calculations, the attraction of the electron density by the localized positron leads to a deepening of the potential well for the positron. This, in turn, leads to an increase of the positron localization in the defect, where the electron density is low. As a result, the two-component DFT gives larger positron lifetimes than calculations in which self-consistency is not imposed.

The present, more precise calculations suggest that the formation of fourfold tetravacancies is the most likely explanation for the apparent disagreement between positron annihilation and infrared spectroscopy data reported in Ref. 27. They also show that the fourfold trivacancy has positron lifetimes close to that for the monovacancy; these two types of defect can thus be confused when interpreting positron annihilation experiments.

ACKNOWLEDGMENTS

The authors are grateful to Rémi Poirier for stimulating discussions and to Ralf Meyer for help with debugging the DFT code. This work was supported by grants from the Natural Sciences and Engineering Research Council (NSERC) of Canada and the "Fonds Québécois de la recherche sur la nature et les technologies" (FQRNT) of the Province of Québec. We are indebted to the "Réseau québécois de calcul de haute performance" (RQCHP) for generous allocations of computer resources.

[1] G. D. Watkins and J. W. Corbett, Phys. Rev. **138**, A543 (1965).
[2] W. Fuhs, U. Holzhauer, S. Mantl, F. W. Richter, and R. Sturm, Phys. Status Solidi B **89**, 69 (1978).
[3] A. Polity, F. Börner, S. Huth, S. Eichler, and R. Krause-Rehberg, Phys. Rev. B **58**, 10 363 (1998).
[4] Y.-H. Lee and J. W. Corbett, Phys. Rev. B **8**, 2810 (1973).
[5] Y.-H. Lee and J. W. Corbett, Phys. Rev. B **9**, 4351 (1974).
[6] M. Huang, Y. Wang, J. Yang, Y. He, Y. Guo, and C. Liu, Mater.

Sci. Forum **105–110**, 1071 (1992).
[7] T. Y. Tan, P. Plekhanov, and U. M. Gösele, Appl. Phys. Lett. **70**, 1715 (1997).
[8] M. J. Puska and R. M. Nieminen, J. Phys. F: Met. Phys. **13**, 333 (1983).
[9] M. J. Puska, Phys. Status Solidi A **102**, 11 (1987).
[10] K. O. Jensen, J. Phys.: Condens. Matter **1**, 10595 (1989).
[11] M. J. Puska, J. Phys.: Condens. Matter **3**, 3455 (1991).
[12] T. E. M. Staab, A. Sieck, M. Haugk, M. J. Puska, T. Frauenheim, and H. S. Leipner, Phys. Rev. B **65**, 115210 (2002).
[13] D. V. Makhov and L. J. Lewis, Phys. Rev. Lett. **92**, 255504 (2004).
[14] E. Boroński and R. M. Nieminen, Phys. Rev. B **34**, 3820 (1986).
[15] M. J. Puska and R. M. Nieminen, Rev. Mod. Phys. **66**, 841 (1994).
[16] J. Arponen and E. Pajanne, Ann. Phys. (N.Y.) **121**, 343 (1979).
[17] M. J. Puska, A. P. Seitsonen, and R. M. Nieminen, Phys. Rev. B **52**, 10 947 (1995).
[18] L. J. Lantto, Phys. Rev. B **36**, 5160 (1987).
[19] D. V. Makhov and L. J. Lewis, unpublished.
[20] L. Gilgien, G. Galli, F. Gygi, and R. Car, Phys. Rev. Lett. **72**, 3214 (1994).
[21] T. Korhonen, M. J. Puska, and R. M. Nieminen, Phys. Rev. B **54**, 15 016 (1996).
[22] P. E. Blöchl, Phys. Rev. B **50**, 17 953 (1994).
[23] G. Kresse and D. Joubert, Phys. Rev. B **59**, 1758 (1999).
[24] M. Saito and A. Oshiyama, Phys. Rev. B **53**, 7810 (1996).
[25] M. J. Puska, S. Mäkinen, M. Manninen, and R. M. Nieminen, Phys. Rev. B **39**, 7666 (1989).
[26] Z. Wang, H. Leipner, R. Krause-Rehberg, V. Bodarenko, and H. Gu, Microelectron. Eng. **66**, 358 (2003).
[27] R. Poirier, V. Avalos, S. Dannefaer, F. Schiettekatte, and S. Roorda, Nucl. Instrum. Methods Phys. Res. B **206**, 85 (2003).